

Structures of small mixed krypton-xenon clusters

Masanari Nagasaka, Nobuhiro Kosugi, and Eckart Rühl

Citation: *The Journal of Chemical Physics* **136**, 234312 (2012); doi: 10.1063/1.4729534

View online: <http://dx.doi.org/10.1063/1.4729534>

View Table of Contents: <http://scitation.aip.org/content/aip/journal/jcp/136/23?ver=pdfcov>

Published by the [AIP Publishing](#)

Articles you may be interested in

Communication: Electron transfer mediated decay enabled by spin-orbit interaction in small krypton/xenon clusters

J. Chem. Phys. **140**, 161103 (2014); 10.1063/1.4873134

Postcollision interaction in noble gas clusters: Observation of differences in surface and bulk line shapes

J. Chem. Phys. **123**, 211101 (2005); 10.1063/1.2135771

Insertion of noble-gas atom (Kr and Xe) into noble-metal molecules (AuF and AuOH): Are they stable?

J. Chem. Phys. **123**, 074323 (2005); 10.1063/1.2000254

The size of neutral free clusters as manifested in the relative bulk-to-surface intensity in core level photoelectron spectroscopy

J. Chem. Phys. **120**, 345 (2004); 10.1063/1.1630027

Structural transitions in metal ion-doped noble gas clusters: Experiments and molecular dynamics simulations

J. Chem. Phys. **108**, 4450 (1998); 10.1063/1.475856



AIP | APL Photonics

APL Photonics is pleased to announce
Benjamin Eggleton as its Editor-in-Chief



Structures of small mixed krypton-xenon clusters

Masanari Nagasaka,¹ Nobuhiro Kosugi,^{1,a)} and Eckart Rühl²

¹*Institute for Molecular Science, Myodaiji, Okazaki 444-8585, Japan and The Graduate University for Advanced Studies, Myodaiji, Okazaki 444-8585, Japan*

²*Physikalische Chemie, Freie Universität Berlin, Takustr. 3, D-14195 Berlin, Germany*

(Received 12 April 2012; accepted 31 May 2012; published online 20 June 2012)

Structures of small mixed krypton-xenon clusters of different compositions with an average size of 30–37 atoms are investigated. The Kr $3d_{5/2}$ and Xe $4d_{5/2}$ surface core level shifts and photoelectron intensities originating from corner, edge, and face/bulk sites are analyzed by using soft x-ray photoelectron spectroscopy. Structural models are derived from these experiments, which are confirmed by theoretical simulation taking induced dipole interactions into account. It is found that one or two small Xe cores are partly embedded in the surface of the Kr clusters. These may grow and merge leading to a phase separation between the two rare gas moieties in mixed clusters with increasing the Xe content. © 2012 American Institute of Physics. [<http://dx.doi.org/10.1063/1.4729534>]

I. INTRODUCTION

Structures of homogeneous rare gas clusters formed by van der Waals interaction¹ are widely investigated by core level excitation and ionization.² Most rare gas clusters with more than 10^3 atoms are found in face-centered cubic (fcc) crystalline structures, the same as the macroscopic solid. Surface and bulk sites of the clusters are clearly distinguished by their chemical shift (surface and bulk core level shift) which is observed in x-ray photoelectron spectroscopy (XPS).^{3–8} The cluster size can be estimated from the expansion conditions⁹ as well as by probing the bulk-to-surface peak ratio by XPS.⁶ On the other hand, small clusters containing less than 200 atoms are mostly found in icosahedral structures, where the surface of the clusters is not close packed.¹⁰ Recently, we have investigated changes in surface structures of small Kr clusters with an average size of up to 30 atoms per cluster by using the high resolution XPS.¹¹ Different surface core level shifts were assigned to different surface sites, such as corner, edge, and face sites. These energy shifts are caused by induction, or polarization of the surrounding atoms induced by a singly charged ion created in the photoionization process.^{12,13} Earlier x-ray absorption work¹⁴ indicated that these different geometric sites correspond to the number of nearest neighbors of the core-excited atom. Recent x-ray absorption¹⁵ and resonant Auger electron¹⁶ work revealed that the exchange interaction of the Rydberg electron with the surrounding atoms has to be taken into account in addition to the induced polarization effect.

Structures of mixed rare gas clusters have been investigated either by co-expansion of two different species or by doping pre-made rare gas clusters by another species. In recent experimental studies, it is discussed that most stable structures in mixed clusters are not obtained from doping.^{17–23} For example, when Ar clusters with an average size of 1000 atoms per cluster are doped by atomic krypton, the krypton is dispersed on the cluster surface and is localized in a

stable way at surface sites.²² Full mixing of these rare gas species is not observed since thermal excitation is not sufficient for diffusion of the Ar atoms. These findings are also confirmed by molecular dynamics calculations.^{24–26}

On the other hand, it is believed that mixed clusters formed by co-expansion can form the most stable structures, as probed by XPS in the size regime of about 10^3 atoms per cluster.^{27–30} Evidently, the surface energy of these clusters is not a dominant factor, due to the small surface contribution in the large cluster regime, and the inter-atomic interactions between different atoms are most important for the formation of energetically stable cluster structures. In mixed Ar-Xe clusters, the Xe atoms tend to be found at bulk sites, whereas the Ar atoms prefer surface sites of the cluster. Such phase segregation in mixed clusters is due to the large difference in cohesive energies between Xe and Ar.^{28,31} Similarly, in mixed Ar-Kr clusters, the krypton is found in the bulk and the argon also covers the surface. However, no complete segregation of both species is observed, where the composition ratio is gradually changed at the border of these core-shell structures.^{28,29,32} This is because the difference in cohesive energy between Ar and Kr is smaller than that between Ar and Xe. Nagaya *et al.*³³ measured x-ray absorption spectra of small mixed Ar-Kr clusters at the Kr K-edge. When the Kr concentration was low, the mixed clusters also showed core-shell structures. Moreover, core-shell structures were also observed in the mixed molecular cluster of CH₄ and CF₄.³⁴

The structure of small mixed clusters is determined by several factors, not only the inter-atomic interaction energies but also the surface energies and the atomic radii. This has not been fully investigated experimentally but has been extensively studied by Monte Carlo simulations.^{35–42} The inter-atomic interactions in rare-gas atoms are well described by Lennard-Jones potentials. Clarke *et al.*³⁶ performed Monte Carlo simulations by changing the interaction energy ϵ in the Lennard-Jones potential, and discussed the dynamics of phase separations between different atoms. The icosahedra are known to have an overall strained structure; however, the associated strain can be removed by choosing the 9.79%

^{a)}Electronic mail: kosugi@ims.ac.jp.

smaller central atoms.⁴³ Doye and Meyer⁴⁰ used the Monte Carlo method by changing the inter-atomic distances σ in the Lennard-Jones potential and confirmed that the cluster structures are changed from polytetrahedra to polyicosahedra as the difference in atomic radii is increased. Calvo and Yurtsever³⁹ investigated the structures of mixed Ar-Xe and Kr-Xe clusters containing 38 atoms by using the Monte Carlo method. The mixed Ar-Xe clusters show icosahedral structures, in which the Ar atoms occupy the bulk sites and are covered by Xe atoms. This is explained by the fact that the atomic radius of Ar is significantly smaller than that of Xe. On the other hand, minimization of the overall strain in mixed Kr-Xe clusters is weak due to the small difference in atomic radius between both species. Small Xe cores in the bulk appear to maximize the interaction energy. The structure of small mixed Kr-Xe clusters is predicted to be a truncated octahedron, which is nearly the same as the fcc crystalline structure.

In the present work, we investigate the structure of small mixed Kr-Xe clusters with an average size of 30–37 atoms by using high resolution XPS. The mixed clusters are produced by co-expansion of gas mixtures of different mixing ratio. We have analyzed the surface core level shift and the relative intensities of XPS signals for different geometrical sites with the help of Monte Carlo simulations and core level shift calculations.

II. METHODS

A. Experiments

The XPS measurements on small mixed Kr-Xe clusters were performed at the soft x-ray in-vacuum undulator beamline BL3U at the storage ring UVSOR-II.⁴⁴ The excitation energies were set to 114.2 and 140.0 eV for studying the Xe $4d_{5/2}$ and Kr $3d_{5/2}$ regimes, respectively. The binding energies of the atomic species are well known, where the Xe $4d_{5/2}$ and Kr $3d_{5/2}$ occur at 67.55 eV and 93.80 eV, respectively.^{6,7} Thus, the kinetic energies of the photoelectrons are almost the same (~ 50.0 eV) for both the Xe $4d_{5/2}$ and Kr $3d_{5/2}$ ionizations. This appears to be surface sensitive with a small attenuation length.⁴⁵ The bandwidth of the incident photons was set to 60 meV for both the inner-shell ionizations. The XPS spectra were measured by using a hemispherical electron energy analyzer (SCIENTA SES-200 combined with an MBS A-1 control system). The analyzer is mounted at $\sim 55^\circ$ to the horizontal polarization plane of the synchrotron radiation (magic angle) for avoiding the angular distribution effect of the electron scattering.⁴⁶ The pass energy was set to 50 eV. The total resolution of the electron energies is ~ 75 meV. The cluster peaks in XPS spectra were observed at the lower binding energies of the atomic signals. The atomic signals were fitted with Voigt profiles, in which the Lorentzian widths are assumed to be 111 meV and 88 meV for the Xe $4d_{5/2}$ and Kr $3d_{5/2}$ regions, respectively. This is essentially due to the core-hole lifetime.⁴⁷ The Gaussian contributions are 68 meV and 79 meV in the Xe $4d_{5/2}$ and Kr $3d_{5/2}$ regions, respectively. The atomic signals were subtracted from the raw XPS spectra in order to analyze exclusively the binding energies in mixed cluster. The binding energy scale was set to be zero for the

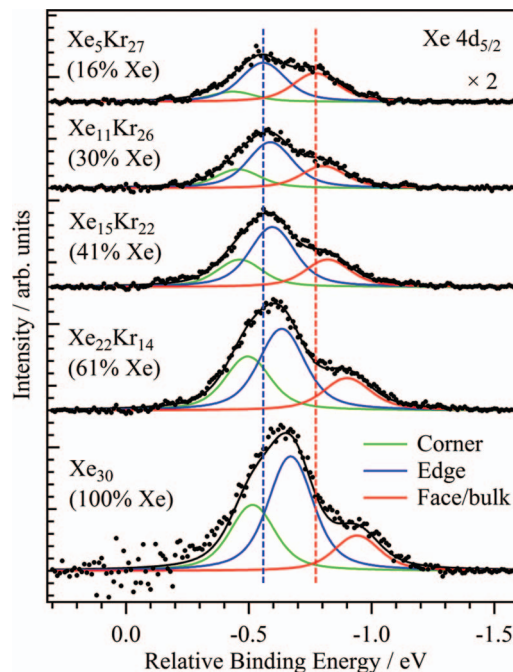


FIG. 1. Xe $4d_{5/2}$ XPS spectra of mixed Kr-Xe clusters. Average Kr and Xe compositions are derived from the Kr $3d_{5/2}$ and Xe $4d_{5/2}$ photoelectron intensities, as shown in Tables I and II. The atomic Xe contribution has been subtracted. The dashed lines indicate the edge and face/bulk sites in Xe₅Kr₂₇ clusters.

atomic species, allowing a comparison of the core level shifts of the cluster peaks shown in Figs. 1 and 2.

Mixed Kr-Xe clusters were formed in a supersonic gas expansion of the primary gas mixtures. The detailed experimental setup was described previously.¹¹ The mixed

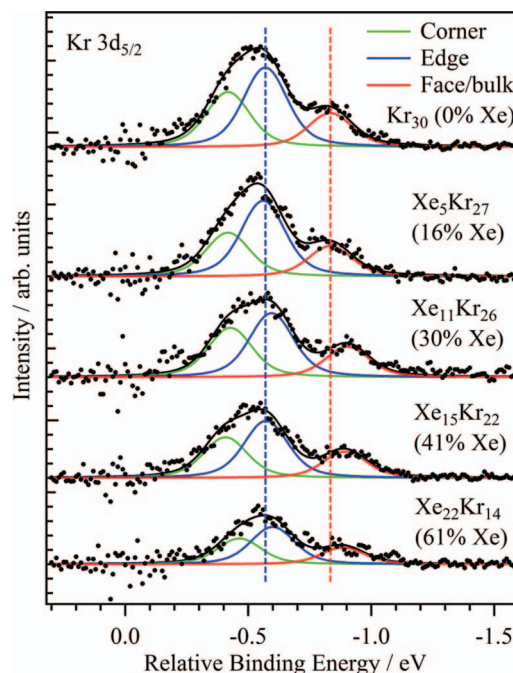


FIG. 2. Kr $3d_{5/2}$ XPS spectra of mixed Kr-Xe clusters. The atomic Kr contribution has been subtracted. The dashed lines indicate the edge and face/bulk sites in Kr₃₀ clusters.

gas containing 1–5 at. % Xe was controlled by a real time gas mixing apparatus (GB-2C, Kofloc Co., Ltd.). The mixed gas was expanded from the nozzle at a temperature of 298 K into the vacuum with a pressure of 0.5 MPa. The average cluster size of Kr clusters was estimated to be 30 atoms per cluster. For the measurement of Xe₃₀ clusters, the total pressure was set to 0.3 MPa, considering the cluster size estimate by Karnbach *et al.*⁹ Clusters grow much larger in xenon expansions than in krypton expansions at identical expansion conditions. Therefore, the fraction of Xe in mixed clusters becomes higher than the mixing ratio in the original gas mixtures.⁴⁸ The composition of the mixed clusters was estimated from the Xe 4*d*_{5/2} and Kr 3*d*_{5/2} XPS-intensities in comparison with that of the homogeneous rare gas clusters with an average size of 30 atoms per cluster. As a result, the average size of the clusters formed from the 1, 2, 3, and 5 at. % Xe mixtures are evaluated as Xe₅Kr₂₇ (16% Xe), Xe₁₁Kr₂₆ (30% Xe), Xe₁₅Kr₂₂ (41% Xe), and Xe₂₂Kr₁₄ (61% Xe), respectively. Danilchenko *et al.* investigated the Xe compositions of the mixed Kr-Xe clusters with an average cluster size of 2000 atoms per cluster by using the electron diffraction method.⁴⁸ They found that the average Xe compositions of the mixed clusters formed from the 2.5 and 5 at. % Xe mixtures are about 20% and 40%, respectively, which are smaller than the present values, ~35% and 61%. This discrepancy could arise from the smaller cluster size studied in this work by two orders of magnitude.

B. Theoretical simulations

The core level shifts at different surface and bulk sites in several structure models of the mixed clusters were derived by taking the induced polarization into account. Model structures were evaluated by considering the size regime studied in the experiments. We performed Monte Carlo simulations using Lennard-Jones potentials. The parameters were taken from the earlier work by Leitner *et al.*,⁴⁹ where the interaction energy ϵ and the inter-atomic distance σ are 164.0 K and 3.826 Å for Kr-Kr interactions and 222.3 K and 4.098 Å for Xe-Xe interactions. The Kr-Xe interactions were derived from the Lorentz-Berthelot combination, yielding ϵ and σ to be 190.9 K and 3.962 Å, respectively. Randomly distributed 35 Kr atoms at 100 K were gradually cooled to 0 K to simulate the formation of stable Kr₃₅ clusters using the Metropolis method.⁵⁰ The aim of the present simulations is not the complete optimization of the global minimum of the structures but is a comparison of some typical stable structure models to simulate the experimental results. Therefore, we used initial guesses, for the optimized structures at 0 K of mixed Kr-Xe clusters, by replacing of some Kr atoms by Xe, where the cluster size was fixed to 35 atoms, considering the average cluster size (30–37) indicated by the experimental results.

The core level shifts at different sites of the mixed clusters were evaluated by considering induced polarization,^{12,13} similar to the earlier work on molecular clusters.^{34,51–53} The atom i near an ionized atom has the induced dipole moment $p = \alpha E$. The polarizability α is 2.48 Å³ for Kr and 4.04 Å³ for Xe.⁵⁴ The electric field vector $E_{i,\mu}$ of the atom i is

described as

$$E_{i,\mu} = E_{i,\mu}^0 - \frac{1}{4\pi\epsilon_0} \sum_{j \neq i}^N \sum_v^3 M_{\mu\nu}(\mathbf{r}_i - \mathbf{r}_j) p_{j,\nu}. \quad (1)$$

The first term in Eq. (1) is the initial electric field caused by the Coulomb interaction of the singly charged ion. The second term is the electric field of the induced dipole moments from surrounding atoms j . The tensor $M_{\mu\nu}(\mathbf{R})$ is described by $M_{\mu\nu}(\mathbf{R}) = (\delta_{\mu,\nu} R^2 - 3R_\mu R_\nu)/R^5$. Since $E_{i,\mu}$ includes the contribution from different atoms j , the solution should be obtained self-consistently. The core level shift S_a at the singly charged ion a is obtained from the sum of the induced dipole moments and the initial electric field as

$$S_a = -\frac{1}{2} \sum_i^N \mathbf{p}_i \cdot \mathbf{E}_i^0. \quad (2)$$

Finally, we summed up the contributions of all atoms a in the cluster to derive the simulated spectra after convolution by a Gaussian profile with a width of 0.2 eV.

III. RESULTS AND DISCUSSION

A. Surface site analysis

Figure 1 shows the Xe 4*d*_{5/2} XPS spectra of Kr-Xe mixed clusters with different composition at an average cluster size of 30–37 atoms per cluster, as outlined in Sec. II A. Different geometrical sites were deconvoluted by a curve fitting procedure using Voigt profiles, similar to the previous work.¹¹ The Gaussian linewidth is set to 150 meV and the Lorentzian width to 111 meV. It is assumed that the clusters are of icosahedral shape containing truncated and distorted local structures. The analyzed energy shifts and the relative intensities of corner, edge, and face/bulk sites of different mixed Kr-Xe clusters are listed in Table I, where the face and bulk sites are clearly blended and were treated as a single peak in the curve fitting procedure. Figure 2 shows the Kr 3*d*_{5/2} XPS spectra for mixed Kr-Xe clusters of different composition. The Lorentzian and Gaussian widths in the curve fitting procedure are set to 88 meV and 160 meV, respectively. The derived energy shifts and peak intensities of the different Kr sites are listed in Table II. In Tables I and II, Xe and Kr atoms at face/bulk sites are shifted by –0.77 eV to –0.94 eV and –0.83 eV to –0.90 eV, respectively. Although such variations might be due to the polarizability of Xe (4.04 Å³), which is larger than that of Kr (2.48 Å³),⁵⁴ the local geometry might

TABLE I. Experimental Xe 4*d*_{5/2} core level shifts (eV) at different sites of the small mixed Kr-Xe and homogeneous Xe clusters relative to the atomic peak as shown in Fig. 1. Total intensities normalized to the Xe₃₀ clusters and the intensity ratios of different sites in parentheses are shown.

Xe 4 <i>d</i> _{5/2}	Total intensity	Corner	Edge	Face/bulk
Xe ₅ Kr ₂₇ (16% Xe)	5.1	–0.43 (13)	–0.56 (50)	–0.77 (37)
Xe ₁₁ Kr ₂₆ (30% Xe)	11.3	–0.46 (22)	–0.59 (53)	–0.80 (25)
Xe ₁₅ Kr ₂₂ (41% Xe)	14.9	–0.46 (24)	–0.60 (52)	–0.82 (24)
Xe ₂₂ Kr ₁₄ (61% Xe)	22.4	–0.50 (31)	–0.63 (49)	–0.90 (20)
Xe ₃₀ (100% Xe)	30	–0.50 (29)	–0.67 (54)	–0.94 (17)

TABLE II. Experimental Kr $3d_{5/2}$ core level shifts (eV) at different sites of the small homogeneous Kr and mixed Kr-Xe clusters relative to the atomic peak as shown in Fig. 2. Total intensities normalized to the Kr₃₀ clusters and the intensity ratios of different sites in parentheses are shown.

Kr $3d_{5/2}$	Total intensity	Corner	Edge	Face/bulk
Kr ₃₀ (0% Xe)	30	-0.42 (33)	-0.57 (47)	-0.83 (20)
Xe ₅ Kr ₂₇ (16% Xe)	26.7	-0.42 (29)	-0.56 (51)	-0.83 (20)
Xe ₁₁ Kr ₂₆ (30% Xe)	25.7	-0.43 (34)	-0.59 (45)	-0.90 (21)
Xe ₁₅ Kr ₂₂ (41% Xe)	22.2	-0.41 (33)	-0.57 (46)	-0.89 (21)
Xe ₂₂ Kr ₁₄ (61% Xe)	14.3	-0.46 (32)	-0.60 (47)	-0.88 (21)

play a dominant role. This is specifically the case, since the ratio of the different Kr sites (corner:edge:face/bulk \approx 3:5:2) is almost independent of the cluster composition, whereas the ratio of the Xe sites is rather dependent on the cluster composition. Note that the XPS spectra do not seem to be influenced by the intensity suppression of the face/bulk sites caused by the inelastic scattering, considering the reasonable intensity ratios of the face/bulk sites.

First, we focus on Xe₂₂Kr₁₄ clusters formed from 5 at. % Xe in the initial gas mixtures, where the resulting ratio of components is Xe:Kr = 61:39 (61% Xe). Figure 1 shows that Xe atoms exist at both the edge and face/bulk sites in these clusters, yielding a core level shift, which is 0.04 eV smaller than that in Xe₃₀ clusters. A decreased core level shift implies that the Xe atoms are in contact with Kr atoms. On the other hand, in the Kr $3d_{5/2}$ XPS spectrum shown in Fig. 2, the Kr face/bulk sites in Xe₂₂Kr₁₄ clusters show a core level shift, which is 0.05 eV larger than that in the Kr₃₀. The Kr corner- and edge-sites also show an enhanced core level shift. This implies that the Kr atoms are also in contact with Xe atoms. If the Xe₂₂Kr₁₄ clusters would have a randomly distributed structure, the absolute core level shifts of Xe and Kr should be almost identical in a finite system. This is unlike the experimental observation, where the surface core level shift of the Xe sites is -0.50, -0.63, and -0.90 eV, whereas that of Kr sites is -0.46, -0.60, and -0.88 eV for corner, edge, and face/bulk sites, respectively. This means that the surroundings of Xe are Xe-rich and the surroundings of Kr sites are Kr-rich, corresponding to a segregated structure. If these Xe₂₂Kr₁₄ clusters would have a core-shell structure with a Xe (Kr) core covered by Kr (Xe) atoms, then the Kr (Xe) face/bulk sites would not be found in the Kr (Xe) XPS spectra. This would also be inconsistent with the present experimental results. The present findings clearly indicate that a phase separation has more or less occurred between the Kr and Xe moieties in Xe₂₂Kr₁₄ clusters, where both the Kr and Xe atoms form substructures, in contact with each other.

Next, we investigate the mixed Xe₅Kr₂₇ clusters (initially 1 at. % Xe gas mixtures), where the resulting ratio of components is Xe:Kr = 16:84 (16% Xe). The Kr $3d_{5/2}$ spectrum is almost the same as that of the Kr₃₀ cluster, as shown in Fig. 2 and Table II. On the other hand, in the Xe $4d_{5/2}$ spectrum shown in Fig. 1 and Table I, all the Xe sites show rather a smaller core level shift than is observed for Xe₃₀: -0.43 eV (corner), -0.56 eV (edge), and -0.77 eV (face/bulk). These values are comparable with the Kr $3d_{5/2}$

level shifts in Kr₃₀: -0.42 eV (corner), -0.57 eV (edge), and -0.83 eV (face/bulk). The smaller Xe $4d_{5/2}$ core level shift at the face/bulk sites is reasonable, if Xe atoms are not completely mixed in krypton but are localized on the surface of the clusters. Furthermore, the ratio of the Xe corner site is rather small. This means that the Xe atoms are not completely on the surface of the Kr moieties but are partly embedded.

Xe₁₁Kr₂₆ clusters (Xe:Kr = 30:70, corresponding to 30% Xe) show a core level shift, which is 0.03 eV larger than that of Xe₅Kr₂₇ clusters (16% Xe), as derived from the Xe $4d_{5/2}$ XPS spectra. The intensity ratio of the Xe corner sites is clearly increased. The core level shift of the Kr face/bulk site is almost the maximum in Xe₁₁Kr₂₆ clusters. These results indicate that the xenon moieties appear to grow while keeping contact with the Kr moieties, and that there is possible replacement of some Kr atoms by Xe atoms at the surface of the clusters. Xe₁₅Kr₂₂ clusters (Xe:Kr = 41:59, corresponding to 41% Xe) show a 0.01–0.02 eV larger Xe $4d_{5/2}$ core level shift and a 0.01–0.02 eV smaller Kr $3d_{5/2}$ core level shift than Xe₁₁Kr₂₆ clusters (30% Xe). The relative intensity ratio in Xe₁₅Kr₂₂ clusters is not changed for both the Kr and Xe sites in comparison with Xe₁₁Kr₂₆ clusters. This implies that the growth of Xe cores continues on the surface of the Kr cluster and these cores are getting in contact with each other and may merge into a larger moiety within the clusters.

B. Comparison with model structures

In order to confirm the experimentally indicated structures of the mixed clusters, core level shifts and intensities of the XPS spectra are simulated by the above-described theoretical approach. Figure 3 shows simulated Xe $4d_{5/2}$ XPS spectra for four different stable structures of Xe₆Kr₂₉ model clusters (17% Xe), which are comparable to Xe₅Kr₂₇ clusters (16% Xe). Note that the experimental size and compositions of the mixed clusters, as discussed in Sec. II A, are average values over size distributions formed by a supersonic expansion. The difference in cluster size and composition between the theoretically chosen values and the experimentally determined ones is small enough to discuss the structure of the mixed clusters by a comparison between the experimental and theoretical results. The results for the Xe₃₅ model cluster are also shown. These spectra are analyzed by using different shifts at the corner, edge, and face/bulk sites, in which the number of the nearest neighbor atoms at the face/bulk site is expected to be 12 and that at the corner site is below 5. The composition ratio of the corner, edge, and face/bulk sites in the simulated spectrum of the Xe₃₅ model clusters are similar to the experimental results shown in Fig. 1. Note that the average number of corner sites is below 1 in Xe₅Kr₂₇ clusters, as indicated in Table I.

First, we discuss model A, in which Kr and Xe atoms are randomly distributed in the mixed clusters. In this case, the intensity of the face/bulk site is smaller than that of the edge sites. In such a small size of mixed clusters, the composition ratio of the face/bulk site is smaller than that of the edge sites. Therefore, Xe atoms should be confined within the mixed clusters in order to reproduce the spectrum for the Xe₅Kr₂₇

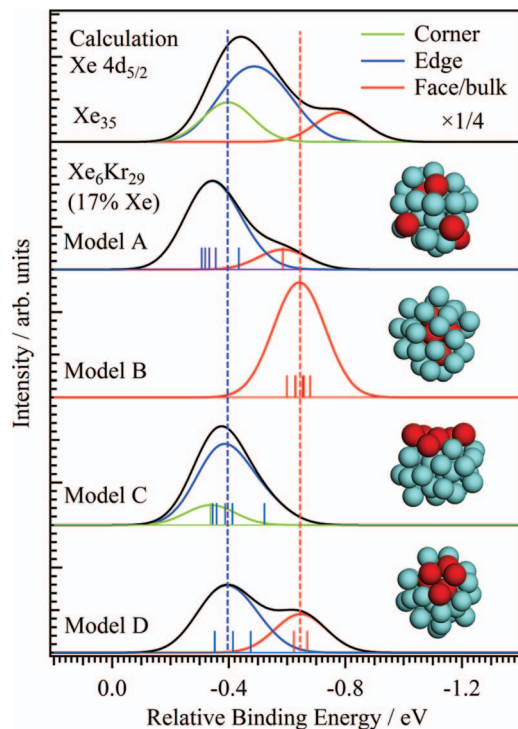


FIG. 3. Calculated Xe $4d_{5/2}$ core level shifts at the corner, edge, and face/bulk sites of four different stable structures of $\text{Xe}_6\text{Kr}_{29}$ model clusters, as well as the Xe_{35} model cluster, where Xe and Kr atoms are indicated by red and green spheres, respectively. Each small vertical bar corresponds to the core level shift of different Xe sites in clusters. The dashed lines indicate the edge and face/bulk sites in model D. The total energy of models B, C, and D relative to that of model A are 0.03 eV, -0.01 eV, and 0.01 eV, respectively.

cluster (16% Xe), in which the intensity of the face/bulk site is higher and close to that of the edge sites. Model B corresponds to a core-shell structure, where the Xe atoms are located at bulk sites and these are covered by Kr atoms. The spectrum of model B shows only the Xe face/bulk sites, which is inconsistent with the experimental results. Note that this structure has an advantage in terms of the higher inter-atomic interaction energy, but there is increased strain due to the large atomic radius of Xe in the central part of the clusters. In model C, a Xe layer is located on the surface of a Kr cluster, and the XPS shows mainly the Xe corner and edge sites. Xe atoms have a large cohesive energy, and tend to stick together. Evidently, the spectrum of model D is in good agreement with the experimental results, where a small Xe cluster is embedded on the surface of a Kr cluster. The relative intensity of the face/bulk sites, as compared to the other surface sites, is 33% in the simulated spectra. This is close to the experimental value of 37%. The core level shifts of the edge and face/bulk sites in model D are 0.09 eV and 0.14 eV smaller than those in homogeneous Xe_{35} clusters, respectively. This is in reasonable agreement with the experimental results of 0.11 eV and 0.17 eV. We have also simulated the Kr $3d_{5/2}$ XPS spectra for Kr_{35} and model D of the $\text{Xe}_6\text{Kr}_{29}$ clusters, as shown in Fig. 4(b). The core level shifts of the surface sites in $\text{Xe}_6\text{Kr}_{29}$ clusters are by 0.02 eV lower than those in the Kr_{35} clusters. The ratio of the different Kr sites is nearly constant between the Kr_{35} and the $\text{Xe}_6\text{Kr}_{29}$. This is consistent with the experimental results, in which the Kr $3d_{5/2}$ XPS spec-

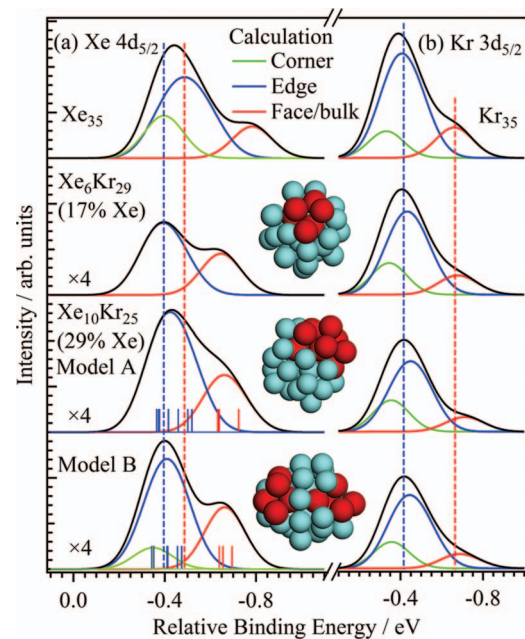


FIG. 4. (a) Calculated Xe $4d_{5/2}$ core level shifts at the corner, edge, and face/bulk sites of two stable structures of $\text{Xe}_{10}\text{Kr}_{25}$ model clusters, as well as the Xe_{35} and $\text{Xe}_6\text{Kr}_{29}$ (model D) model clusters, where Xe and Kr atoms are indicated by red and green spheres, respectively. Each small vertical bar corresponds to the core level shift of different Xe sites in clusters. The dashed lines indicate the edge sites in Xe_{35} and $\text{Xe}_6\text{Kr}_{29}$ (model D) model clusters. The total energy of model A is by 0.05 eV lower than that of model B. (b) Calculated Kr $3d_{5/2}$ core level shifts at the different sites of the mixed model clusters that are the same as (a). The dashed lines indicate the edge and face/bulk sites in Kr_{35} model clusters.

trum of $\text{Xe}_5\text{Kr}_{27}$ clusters is almost the same as that of Kr_{30} clusters.

Figure 4(a) shows the simulated Xe $4d_{5/2}$ XPS spectra for two different stable structures of $\text{Xe}_{10}\text{Kr}_{25}$ model clusters (29% Xe), to be compared with the $\text{Xe}_{11}\text{Kr}_{26}$ cluster (30% Xe). The estimated number of Xe corner sites is 2, as indicated in Table I. Figure 4(a) also shows simulated spectra of Xe_{35} and $\text{Xe}_6\text{Kr}_{29}$ (17% Xe) model clusters for comparison. The structures of models A and B consist of a Xe_{10} cluster core and two Xe_5 cores embedded in the Kr cluster, respectively. The core level shift of the face/bulk sites in models A and B is not different from each other. However, the Xe core level shifts at the edge sites in models A and B are 0.03 eV and 0.02 eV larger than those of the $\text{Xe}_6\text{Kr}_{29}$ model clusters (17% Xe), respectively. The experimental Xe core level shifts of the edge site in $\text{Xe}_{11}\text{Kr}_{26}$ clusters (30% Xe) are 0.03 eV larger than in the $\text{Xe}_5\text{Kr}_{27}$ clusters (16% Xe). The number of Xe corner site in the two Xe_5 cores is larger than that in the single Xe_{10} core. The experimental intensity of the corner sites in $\text{Xe}_{11}\text{Kr}_{26}$ clusters is larger than that in $\text{Xe}_5\text{Kr}_{27}$ clusters. This implies that the single Xe_{10} core in $\text{Xe}_{10}\text{Kr}_{25}$ model clusters underestimates the intensity of the corner sites; on the other hand, the two Xe_5 cores model underestimates the core level shift of the edge sites. Therefore, it appears to be likely that $\text{Xe}_{11}\text{Kr}_{26}$ clusters might have a structure which is between the models A and B. The simulated Kr $3d_{5/2}$ XPS spectra shown in Fig. 4(b) also confirm these structures. The face/bulk sites of models A and B in the $\text{Xe}_{10}\text{Kr}_{25}$ clusters show by

0.05 eV and 0.03 eV larger energy shifts from those of the Kr_{35} clusters, respectively, as observed in $\text{Kr } 3d_{5/2}$ XPS spectra. This means that Kr atoms are in contact with Xe atoms at the face/bulk sites of the mixed clusters. This is reasonable, considering that the Kr moiety with a smaller atomic radius prefers a more closed packed structure and some vacancies on the Kr surface are occupied by a few Xe sites, and that the mixed Kr-Xe clusters are theoretically predicted to show a transition from icosahedra to the fcc lattice of the crystal by doping with Xe atoms.³⁹

Total energies of the different model structures were also calculated. For $\text{Xe}_6\text{Kr}_{29}$ model clusters (17% Xe), the total energies of the models B, C, and D relative to that of model A are 0.03 eV, -0.01 eV, and 0.01 eV, respectively. The total energy of model A in the $\text{Xe}_{10}\text{Kr}_{25}$ model clusters (29% Xe) is by 0.05 eV lower than that of model B. The differences in total energy between the different cluster models are evidently too small to derive reasonable structure models simulating the experimental spectra.

Figure 5 summarizes the structure models of the proposed mixed Kr-Xe clusters at different mixing ratios of the rare gases. As shown in Fig. 5(a), the homogeneous Kr_{35} model cluster prefers an icosahedron-like structure, in which the surface of the cluster is not a closed packed structure in order to lower the surface energy. In $\text{Xe}_6\text{Kr}_{29}$ model clusters (17% Xe), as shown in Fig. 5(b), a small Xe cluster core is embedded on the surface of the Kr cluster. By increasing the mixing ratio of Xe atoms, one or two small Xe clusters are embedded on the surface of the larger Kr cluster in $\text{Xe}_{10}\text{Kr}_{25}$ model clusters (29% Xe) as shown in Figs. 5(c) and 5(d).

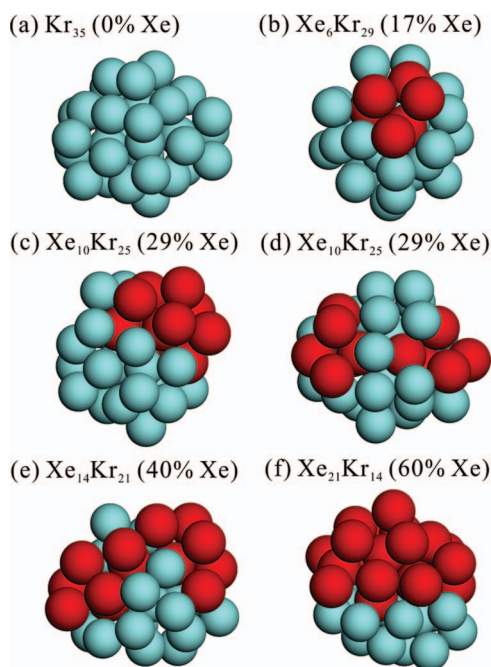


FIG. 5. Proposed model structures of mixed Kr-Xe clusters of different composition, where the cluster size is fixed to 35 atoms. (a) The homogeneous Kr_{35} cluster, (b) $\text{Xe}_6\text{Kr}_{29}$ cluster, (c) $\text{Xe}_{10}\text{Kr}_{25}$ cluster containing a single Xe cluster and (d) two small Xe clusters are contained in $\text{Xe}_{10}\text{Kr}_{25}$ clusters, (e) $\text{Xe}_{14}\text{Kr}_{21}$ cluster, and (f) $\text{Xe}_{21}\text{Kr}_{14}$ cluster, which is comparable to the experimental mixed Kr-Xe clusters.

The vacancies on the surface of the Kr clusters are filled by a few Xe atoms, and the surface of the Kr clusters shows a more closed packed structure. We have calculated the average distance between the Kr atoms at the surface sites of the clusters. These are found to be 4.38 Å and 4.30 Å in Kr_{35} and $\text{Xe}_{21}\text{Kr}_{14}$ model clusters (60% Xe), respectively. These results confirm the formation of close packed Kr structure by doping with Xe. Figure 5(e) indicates the $\text{Xe}_{14}\text{Kr}_{21}$ model cluster (40% Xe). The Kr atoms at the surface sites are replaced by Xe atoms so that no additional Xe can be accommodated. Therefore, the small Xe clusters can be in contact with each other on the surface, and are merged into a larger Xe cluster. Finally, the phase separation between Xe and Kr moieties occurs in $\text{Xe}_{21}\text{Kr}_{14}$ model clusters (60% Xe), as shown in Fig. 5(f). This phase separation is caused by different interaction energy potential of Xe from that of Kr, and has also been deduced from previous Monte Carlo simulations.³⁹

IV. CONCLUSIONS

The structures of small mixed rare gas clusters depend critically on the atomic composition. Surface core level shifts in XPS reveal structural changes in variable size mixed clusters, where the chemical environment of the surface sites varies with the number of nearest neighbor atoms in small mixed clusters. In the present work, we have measured the $\text{Xe } 4d_{5/2}$ and $\text{Kr } 3d_{5/2}$ XPS for mixed Kr-Xe clusters. Co-expansion of 1, 2, 3, and 5 at. % Xe mixtures in gaseous Kr is found to yield mixed clusters with an average size of 30–37 atoms per cluster: $\text{Xe}_5\text{Kr}_{27}$ (16% Xe), $\text{Xe}_{11}\text{Kr}_{26}$ (30% Xe), $\text{Xe}_{15}\text{Kr}_{22}$ (41% Xe), and $\text{Xe}_{22}\text{Kr}_{14}$ (61% Xe), respectively, according to the analysis of the XPS signal intensities.

The experimental cluster XPS-peaks are analyzed by a curve fitting procedure for different geometrical sites, i.e., corner, edge, and face/bulk sites similar to a previously developed method, where homogeneous clusters were investigated.^{11,14–16} Structures of mixed Kr-Xe clusters are derived from the atomic composition dependence of the core level shifts and intensities of XPS-features for each surface site. These structures are confirmed by theoretical simulations taking the induced dipole interaction into account. A small Xe core is embedded on the surface of a Kr cluster in mixed $\text{Xe}_5\text{Kr}_{27}$ clusters (16% Xe). By increasing the Xe mixing ratio in the jet expansion, one or two small Xe clusters are embedded on the surface of a larger Kr cluster in $\text{Xe}_{11}\text{Kr}_{26}$ clusters (30% Xe). It is known that small Kr clusters in the size regime below 200 atoms yield preferably icosahedral structures.¹⁰ Thus, the cluster surface is not a closed packed structure with the minimum surface energy. When Xe atoms are doped in a larger Kr cluster, vacancies on the surface of the Kr cluster are filled by Xe atoms and the cluster shows a fcc-like closed packed structure. Such a transition from an icosahedron-like to a fcc-like closed-packed structure is also consistent with results from Monte Carlo simulations.³⁹ In $\text{Xe}_{15}\text{Kr}_{22}$ clusters (41% Xe), small Xe clusters can get contact with each other and may merge into a larger moiety of Xe atoms. Finally, the full phase separation between Xe and Kr moieties is found for $\text{Xe}_{22}\text{Kr}_{14}$ cluster (61% Xe).

ACKNOWLEDGMENTS

Part of this work is supported by the Japan Society for the Promotion of Science (JSPS) Grant-in-Aids for Scientific Research (Nos. 19850029 and 20350014). Financial support by Deutsche Forschungsgemeinschaft (DFG) (Grant No. RU 420/8-1) is gratefully acknowledged. The authors would like to acknowledge kind supports by the staff members of the UVSOR-II facility.

- ¹ *Clusters of Atoms and Molecules*, edited by H. Haberland (Springer, Berlin, 1994).
- ² E. Rühl, *Int. J. Mass Spectrom.* **229**, 117 (2003).
- ³ O. Björneholm, F. Federmann, F. Fössing, and T. Möller, *Phys. Rev. Lett.* **74**, 3017 (1995).
- ⁴ R. Feifel, M. Tchapyguine, G. Öhrwall, M. Salonen, M. Lundwall, R. R. T. Marinho, M. Gisselbrecht, S. L. Sorensen, A. Naves de Brito, L. Karlsson, N. Mårtensson, S. Svensson, and O. Björneholm, *Eur. Phys. J. D* **30**, 343 (2004).
- ⁵ G. Öhrwall, M. Tchapyguine, M. Lundwall, R. Feifel, H. Bergersen, T. Rander, A. Lindblad, J. Schulz, S. Peredkov, S. Barth, S. Marburger, U. Hergenbahn, S. Svensson, and O. Björneholm, *Phys. Rev. Lett.* **93**, 173401 (2004).
- ⁶ M. Tchapyguine, R. R. Marinho, M. Gisselbrecht, J. Schulz, N. Mårtensson, S. L. Sorensen, A. Naves de Brito, R. Feifel, G. Öhrwall, M. Lundwall, S. Svensson, and O. Björneholm, *J. Chem. Phys.* **120**, 345 (2004).
- ⁷ M. Lundwall, R. F. Fink, M. Tchapyguine, A. Lindblad, G. Öhrwall, H. Bergersen, S. Peredkov, T. Rander, S. Svensson, and O. Björneholm, *J. Phys. B* **39**, 5225 (2006).
- ⁸ D. Rolles, H. Zhang, Z. D. Pešić, R. C. Bilodeau, A. Wills, E. Kukk, B. S. Rude, G. D. Ackerman, J. D. Bozek, R. Díez Muiño, F. J. García de Abajo, and N. Berrah, *Phys. Rev. A* **75**, 031201 (2007).
- ⁹ R. Karnbach, M. Joppien, J. Stapelfeldt, J. Wörmer, and T. Möller, *Rev. Sci. Instrum.* **64**, 2838 (1993).
- ¹⁰ S. Kakar, O. Björneholm, J. Weigelt, A. R. B. de Castro, L. Tröger, R. Frahm, T. Möller, A. Knop, and E. Rühl, *Phys. Rev. Lett.* **78**, 1675 (1997).
- ¹¹ T. Hatsui, H. Setoyama, N. Kosugi, B. Wassermann, I. L. Bradeanu, and E. Rühl, *J. Chem. Phys.* **123**, 154304 (2005).
- ¹² G. J. Martyna and B. J. Berne, *J. Chem. Phys.* **90**, 3744 (1989).
- ¹³ O. Björneholm, F. Federmann, F. Fössing, T. Möller, and P. Stampfli, *J. Chem. Phys.* **104**, 1846 (1996).
- ¹⁴ A. Knop, B. Wassermann, and E. Rühl, *Phys. Rev. Lett.* **80**, 2302 (1998).
- ¹⁵ M. Nagasaka, T. Hatsui, and N. Kosugi, *J. Electron Spectrosc. Relat. Phenom.* **166–167**, 16 (2008).
- ¹⁶ M. Nagasaka, T. Hatsui, H. Setoyama, E. Rühl, and N. Kosugi, *J. Electron Spectrosc. Relat. Phenom.* **183**, 29 (2011).
- ¹⁷ T. Laarmann, K. von Haefen, A. Kanaev, H. Wabnitz, and T. Möller, *Phys. Rev. B* **66**, 205407 (2002).
- ¹⁸ T. Laarmann, K. von Haefen, H. Wabnitz, and T. Möller, *Surf. Rev. Lett.* **9**, 111 (2002).
- ¹⁹ T. Laarmann, K. von Haefen, H. Wabnitz, and T. Möller, *J. Chem. Phys.* **118**, 3043 (2003).
- ²⁰ A. Kanaev, L. Museum, F. Edery, T. Laarmann, and T. Möller, *Phys. Rev. B* **69**, 125343 (2004).
- ²¹ A. Lindblad, H. Bergersen, T. Rander, M. Lundwall, G. Öhrwall, M. Tchapyguine, S. Svensson, and O. Björneholm, *Phys. Chem. Chem. Phys.* **8**, 1899 (2006).
- ²² M. Lundwall, A. Lindblad, H. Bergersen, T. Rander, G. Öhrwall, M. Tchapyguine, S. Svensson, and O. Björneholm, *J. Chem. Phys.* **125**, 014305 (2006).
- ²³ R. von Pietrowski, K. von Haefen, T. Laarmann, T. Möller, L. Museum, and A. V. Kanaev, *Eur. Phys. J. D* **38**, 323 (2006).
- ²⁴ H. Vach, *J. Chem. Phys.* **111**, 3536 (1999).
- ²⁵ H. Vach, *Phys. Rev. B* **59**, 13413 (1999).
- ²⁶ H. Vach, *J. Chem. Phys.* **113**, 1097 (2000).
- ²⁷ M. Lundwall, M. Tchapyguine, G. Öhrwall, R. Feifel, A. Lindblad, A. Lindgren, S. Sörensen, S. Svensson, and O. Björneholm, *Chem. Phys. Lett.* **392**, 433 (2004).
- ²⁸ M. Tchapyguine, M. Lundwall, M. Gisselbrecht, G. Öhrwall, R. Feifel, S. Sorensen, S. Svensson, N. Mårtensson, and O. Björneholm, *Phys. Rev. A* **69**, 031201 (2004).
- ²⁹ M. Lundwall, H. Bergersen, A. Lindblad, G. Öhrwall, M. Tchapyguine, S. Svensson, and O. Björneholm, *Phys. Rev. A* **74**, 043206 (2006).
- ³⁰ M. Lundwall, W. Pokapanich, H. Bergersen, A. Lindblad, T. Rander, G. Öhrwall, M. Tchapyguine, S. Barth, U. Hergenbahn, S. Svensson, and O. Björneholm, *J. Chem. Phys.* **126**, 214706 (2007).
- ³¹ Y. S. Doronin and V. N. Samovarov, *Opt. Spectrosc.* **102**, 906 (2007).
- ³² E. Fort, H. Vach, M. Châtelet, A. De Martino, and F. Pradère, *Eur. Phys. J. D* **14**, 71 (2001).
- ³³ K. Nagaya, H. Murakami, H. Iwayama, and M. Yao, *J. Electron Spectrosc. Relat. Phenom.* **166–167**, 11 (2008).
- ³⁴ M. Winkler, J. Harnes, and K. J. Børve, *J. Phys. Chem. A* **115**, 13259 (2011).
- ³⁵ D. H. Robertson, F. B. Brown, and I. M. Navon, *J. Chem. Phys.* **90**, 3221 (1989).
- ³⁶ A. S. Clarke, R. Kapral, B. Moore, G. Patey, and X.-G. Wu, *Phys. Rev. Lett.* **70**, 3283 (1993).
- ³⁷ D. D. Frantz, *J. Chem. Phys.* **107**, 1992 (1997).
- ³⁸ L. J. Munro, A. Tharrington, and K. D. Jordan, *Comput. Phys. Commun.* **145**, 1 (2002).
- ³⁹ F. Calvo and E. Yurtsever, *Phys. Rev. B* **70**, 045423 (2004).
- ⁴⁰ J. P. K. Doye and L. Meyer, *Phys. Rev. Lett.* **95**, 063401 (2005).
- ⁴¹ R. P. White, S. M. Cleary, and H. R. Mayne, *J. Chem. Phys.* **123**, 094505 (2005).
- ⁴² S. M. Cleary and H. R. Mayne, *Chem. Phys. Lett.* **418**, 79 (2006).
- ⁴³ S. Cozzini and M. Ronchetti, *Phys. Rev. B* **53**, 12040 (1996).
- ⁴⁴ T. Hatsui, E. Shigemasa, and N. Kosugi, *AIP Conf. Proc.* **705**, 921 (2004).
- ⁴⁵ M. P. Seah and W. A. Dench, *Surf. Interface Anal.* **1**, 2 (1979).
- ⁴⁶ H. Zhang, D. Rolles, Z. D. Pešić, J. D. Bozek, and N. Berrah, *Phys. Rev. A* **78**, 063201 (2008).
- ⁴⁷ M. Jurvansuu, A. Kivimäki, and S. Aksela, *Phys. Rev. A* **64**, 012502 (2001).
- ⁴⁸ A. G. Danilchenko, S. I. Kovalenko, A. P. Konotop, and V. N. Samovarov, *Low Temp. Phys.* **37**, 532 (2011).
- ⁴⁹ D. M. Leitner, J. D. Doll, and R. M. Whitnell, *J. Chem. Phys.* **94**, 6644 (1991).
- ⁵⁰ N. Metropolis, A. W. Rosenbluth, M. N. Rosenbluth, A. H. Teller, and E. Teller, *J. Chem. Phys.* **21**, 1087 (1953).
- ⁵¹ M. Abu-Samha, K. J. Børve, L. J. Sæthre, G. Öhrwall, H. Bergersen, T. Rander, O. Björneholm, and M. Tchapyguine, *Phys. Chem. Chem. Phys.* **8**, 2473 (2006).
- ⁵² M. Abu-Samha and K. J. Børve, *J. Chem. Phys.* **128**, 154710 (2008).
- ⁵³ J. Harnes, M. Abu-Samha, M. Winkler, H. Bergersen, L. J. Sæthre, and K. J. Børve, *J. Electron Spectrosc. Relat. Phenom.* **166–167**, 53 (2008).
- ⁵⁴ T. M. Miller and B. Bederson, *Adv. At. Mol. Phys.* **13**, 1 (1978).